Special Series

Experimental Methods in Chemical Engineering: Temperature Programmed Reduction—TPR[†]

Carlo Pirola[a], Federico Galli[a], Gregory S. Patience[b]

[a] Department of Chemistry, Universitá degli Studi di Milano, via Golgi 19, 20133 Milano Italy

[b]Department of Chemical Engineering, Polytechnique Montréal, C.P. 6079, Succ. CV Montréal, H3C 3A7, Québec, Canada

Abstract

Temperature programmed reduction (TPR) characterizes the oxido-reduction properties of bulk and supported catalysts. H_2 or CO pass over a pre-conditioned solid sample as a furnace ramps the temperature at a constant rate. A thermal conductivity detector (TCD) or mass spectrometer records the effluent concentration. In the pre-conditioning step, Ar or He flushes residual air and absorbed water from the solids sample to maximize the signal-to-noise ratio of the TCD signal. We calculate the number of active sites based on the detector signal that correlates with how much hydrogen reacts. The temperature at which it begins to react represents the minimum activation temperature. TPR is cheap, fast, easy to run, and the data is straightforward to interpret. The technique is more popular with chemical engineers than with the broader scientific community. Among the 27 articles that *Can. J. Chem. Eng.* published in 2016 and 2017[1] that apply TPR to analyze catalysts, 22 mention reactors, 20 report XRD spectra, 18 mention gas chromatography, and another 15 quantify surface area by BET. Synergy with other temperature programmed methods is lower, as only 5 mention temperature programmed desorption, 5 thermal gravimetric analysis, and 3 temperature programmed oxidation.This article is protected by copyright. All rights reserved

INTRODUCTION

Temperature programmed reduction (TPR) belongs to a class of chemical techniques to evaluate how readily hydrogen or CO reduces the oxidation state of solids and in particular catalysts.[2] TPR continues to gain prominence to characterize both bulk and supported metal heterogeneous catalysts,[3] as it gauges the oxido-reduction properties of metals as a function of temperature. According to our map of analytical techniques it falls under the last column of activities *bulk/morphology* and the last row, which we assign to *reactivity*.[4, 5, 6] However, the technique identifies changing oxidation states, which relates to the top row and first column *bulk/nature of the phases*.

Description

A stream of H_2 or CO in N_2 or He (with a mole fraction from 3% to 15%) sweeps across a bed of solids contained in a quartz tube. A high aspect ratio (high length to diameter) maximizes the contact between the gas and solids thereby minimizing radial and thermal gradients. Typically the tube diameter is ¡ 20 mm. A thermocouple placed in the bed monitors the temperature rise as an electrical furnace ramps it up at a rate from $1\,K \cdot min^{-1}$ to $20\,K \cdot min^{-1}$. A thermal conductivity detector (TCD) or mass spectrometer (MS) monitors the effluent gas concentration continuously and changes in the signal correspond to a change in the oxidation state (Figure 1). (Eq. 1).
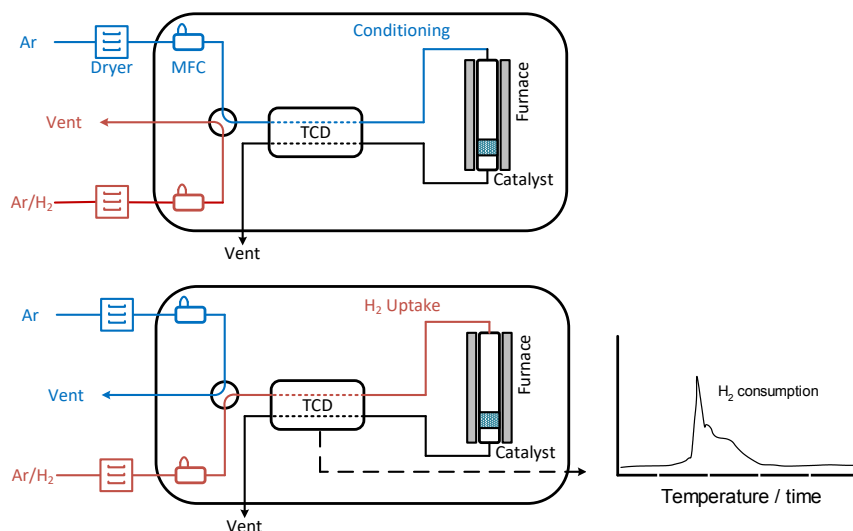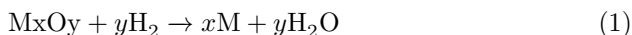
$$MxOy + yH_2 \rightarrow xM + yH_2O \qquad (1)$$

Figure 1: TPR instrument conditioning and H_2 uptake sequence.

TPR determines the energetic nature of catalysts[7] and it identifies the temperature required to activate the metallic phase. Here we report two TPR curves of a 10% by weight iron supported on silica (Figure 2a) and the same sample with Cu and K loaded as promoters (3.75% and 5.65% by weight respectively). A Thermoquest Mod. TPR/D/O 1100 instrument performed the analyses. The samples were pre-treated in a flow of argon at $473\,K$ for $0.5\,h$. After cooling to $323\,K$, the H_2/Ar ($2.28\,g \cdot L^{-1}$) reducing mixture flowed through the sample ($0.030\,g$) at $30\,mL \cdot min^{-1}$ and the temperature ramped from $323\,K$ to $1173\,K$ at a constant rate of $8\,K \cdot min^{-1}$.

The iron phase transformation proceeds in two stages: from hematite (Fe_2O_3) to magnetite (Fe_3O_4) and then magnetite to metallic iron (second broad peak of Figure 2a). The large peak width of this last transformation indicates that this reaction is slower than the former. The peak corresponding to the reduction of

2
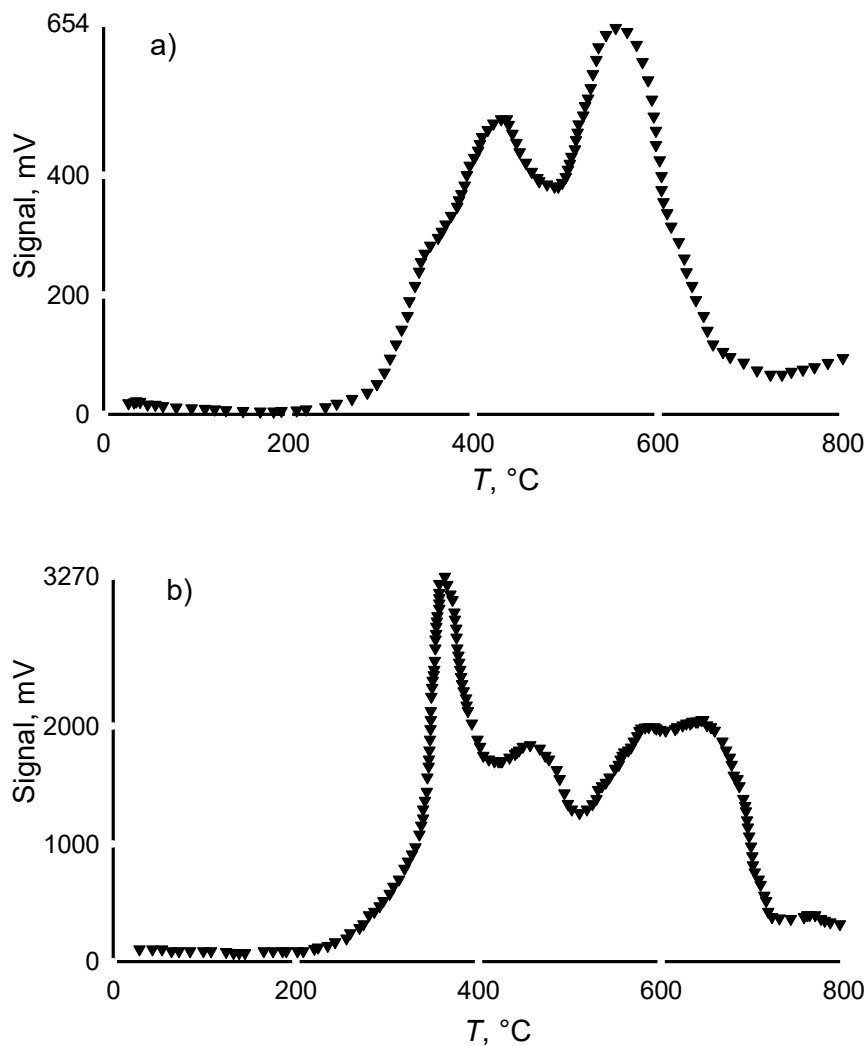
Figure 2: TPR traces of: a) a Fe/SiO$_2$, and b) a Cu−K promoted Fe/SiO$_2$ catalysts.

CuO to Cu is also present at a lower temperature, and it partially overlaps the iron transformations (Figure 2b). Copper promotes the reduction from hematite to magnetite, and also, the reduction from magnetite to a-Fe to a lower extent. TPR shows that metal reduction starts at about 260 °C for the unpromoted catalyst and at about 230 °C for the promoted one. Moreover, promotion shifts the iron oxide reduction reactions to lower temperatures. Cu therefore improves the reduction of iron oxide phases because it migrates atomic hydrogen from reduced Cu sites to the iron oxide.[8]

3

The activation step is critical for several processes to produce selective catalyst like for Fischer-Tropsch synthesis.[9, 10] Scientists and engineers study the role of preparation procedure, (time, temperature, and hydrogen partial pressure, for example), promoters, dopants, and stabilizing agents to enhance catalyst stability, activity, and yield. The TPR protocol first pre-treats the sample and then exposes it to a specified hydrogen flow while ramping the temperature of the furnace according to a set program. Pre-treating the sample increases the reproducibility of the test. It involves passing pure or diluted oxygen to the reactor, which reacts with carbonaceous species and other contaminants deposited on the solid and raises the oxidation state. In the next step, adsorbed water desorbs while the furnace maintains the reactor at $120\,°C$ to $160\,°C$ in vacuum or in a stream of inert gas.

After the sample is sufficiently conditioned, the instrument initates hydrogen or CO flow while ramping up the temperature at a fixed rate until it reaches the set-point. The furnace maintains the maximum temperature for a prescribed time or until the operator is satisfied that the sample is fully reduced. The TPR results (peak shape, resolution of reduction steps, and maximum reduction temperature) establishes a suitable activation procedure to optimize catalyst performance and estimates the expected catalyst activity.

Several factors may affect TPR experiments, either belonging to the sample or to the analysis procedure. The sample bias sources are the presence of contaminants, the amount and distribution of active metals and the size of the catalyst particles. On the other hand, hydrogen concentration in the reducing stream, gas flowrate, and the temperature heating ramp are the parameters of the instrument to optimize.[7, 11]

APPLICATIONS

The Web of Science Core Collection (WoS) indexed 2932 documents in 2016 and 2017 that contained *temperature programmed reduction* or *TPR* under the basic search category *Topic*. Chemical engineering was the second most active category with 826 articles after physical chemistry with 1139. VOSviewer[12] created a word map based on *Title* and *Abstract* as unit analysis (Figure 3). TPR characterizes nanomaterials and catalysts for selective hydrogenation (green), catalysts for CO_2, biomass or glycerol reduction, mainly based on Ni as the active phase (blue), which is tightly connected to the Fischer-Tropsch reaction (CO hydrogenation to give hydrocarbons, as shown in the yellow cluster). The red cluster aggregates the most common keywords, namely reduction, oxidation, and oxide catalyst, that are in articles that mention TPR. Raman spectroscopy is the only characterization technique cited apart from TPR (green cluster). Raman reveals changes in the molecular structure of a material and complements the information that TPR provides. The topic with the most category interconnections is applied science.

Generally, engineers employ TPR to identify optimal reduction conditions for a catalyst, e.g., for Fisher-Tropsch,[13, 14, 15] hydrogenation, dehydrogenation, and hydrodeoxygenation,[16, 17, 18, 19] reverse water gas shift reactions,[20]

4

Figure 3: Citation analysis for TPR, 2015–2017, source: Web of Science.

and reforming[21, 22] catalysts. Rives et al. [23] characterized anionic clays by reducing the different cations included in the matrix structure. Ansaloni et al. [24] elucidated the mechanism of the hydrodeoxygenation of guaiacol over molybdenum-based catalysts with TPR. de Caprariis et al. [25] evaluated the Ni dispersion over diverse catalysts from TPR data. First, they calculated hydrogen adsorption at room temperature and then the metal dispersion with the hypothesis of homologous hydrogen adsorption:[26] (Eq. 2)

$$\text{Ni}_{\text{,dispersion}} = 2 \cdot \frac{\text{H}_{2,\text{adsorbed}}}{\text{H}_{2,\text{consumed}}} \tag{2}$$

UNCERTAINTY

Sources of Errors and Limitations

The most important sources of error for TPR analysis might derive from the pre-treatment procedure and the presence of water adsorbed on the catalyst's surface. Moreover, the size of metal clusters and the active phase loading should be properly considered. Each catalyst requires specific conditions to make the following reduction reproducible. Low temperature and short pre-treatment times may be insufficient to remove all impurities. However, high temperatures sinter active sites. As a general rule-of-thumb, we suggest a temperature in

5

the range of $120\,°C$ to $140\,°C$ for $2\,h$ to $3\,h$ for conditioning. Adsorbed water on catalysts initiates hydrogenation at a lower temperature compared to dry samples. Consequently, we observe a shift of the metal reduction peaks from $5\,°C$ to $10\,°C$. The characteristic reduction temperature of a sample corresponds to the maximum of the TCD peak, and it depends on the size of the metal aggregates on the support. The bigger the size of these clusters, the greater the shift of the reduction temperature peak. Similarly, the quantity of metal loaded on a catalyst affects the thermogram. In fact, at a higher metal loading, aggregates are generally larger and the metal-support interactions change the catalyst behaviour during the analysis. For example, Fadoni and Lucarelli[27, 28] reported the TPR of a Ni/SiO_2 catalyst. With a Ni mass fraction of $26\,\%$, the first reduction peak appears at $320\,°C$. When the loading increased to a mass fraction of $29\,\%$, the same peak shifted to $330\,°C$. Diverse supports lead to dissimilar results, i.e., Ni/SiO_2 features two reduction peaks, whereas a TPR of Ni/Al_2O_3 has three additional peaks. Malet and Caballero[7] formulated the parameter P (Eq. 3), expressed in K, to assess whether the thermogram is influenced by the experimental configuration.

$$P = \frac{\beta \cdot S_0}{F \cdot C_0} \leq 20\,K \tag{3}$$

where β is the heating rate ($K \cdot min^{-1}$), S_0 is the initial catalyst mass (g), F is the carrier flow rate ($L \cdot min^{-1}$), and C_0 is the hydrogen concentration at the reactor inlet ($g \cdot L^{-1}$). P value should be lower than $20\,K$ and as low as possible within the sensitivity of the instrument. As an example, the P parameter for the TPR reported in Figure 2 is $3.5\,K$, and that supports the recommendation to operate at $P < 20\,K$.

Detection Limits

TPR instruments come with thermal conductivity detectors (TCD), which are robust, reliable, and inexpensive. The TCD records an electrical signal that corresponds to the change in composition between a reference gas and the effluent and reports the data as mV or µV. The standard effluent concentration ranges from $5\,µL \cdot L^{-1}$ to $50\,µL \cdot L^{-1}$. A stable flow rate and minimizing dead zones (stagnant regions) improve the sensitivity. Monti and Baiker[11] proposed two criteria to achieve an acceptable signal to noise ratio: a) the hydrogen consumed (at the maximum peak) should always be less than the $66\,\%$ of the H_2 fed; and b) the minimum H_2 conversion should be $10\,\%$. Furthermore, a linear heating rate, scavenging all water upstream of the detector with suitable traps, and an excellent electrical connection[27, 28] are the main factors to achieve good reproducibility. Instruments with optimal sensitivity require smaller samples in the reactor, which minimizes re-adsorption and diffusional limitations. From the thermograph we derive the hydrogen uptake corresponding to each reduction peak then calculate the mass of metal reduced.

TPR reproducibility depends on the pre-treatment procedure and the operating conditions (P parameter). The reduction profile may be considered as a

6

semi-quantitative result, as we often compare it to a reference or other known sample profiles. The H_2 uptake is a quantitative result particularly for $P < 20\,\mathrm{K}$. The work of Alamolhoda et al. [29] is an excellent example where the authors compared several Ce$-$Ni–MFI catalysts for the water gas shift at $P = 15\,\mathrm{K}$. They measured 16 TPR profiles—one for each catalyst composition—to identify the maximum reduction temperature. Moreover, they examined the relationship between composition and hydrogen consumption. Together with identifying the optimal catalyst composition, it identified morphology changes with time-on-stream in the reactor. Metals sinter and agglomerate due physico-chemical phenomena, like cycling temperature, reaction, and mechanical stresses. TPR measures how H_2 uptake over a sample varies with time and operating conditions from which we calculate changes in metal availability. Operating the catalyst beyond the standard operating temperature is one means to devise an accelerated aging test to differentiate between catalysts.

CONCLUSIONS

TPR characterizes catalytic materials and it defines their optimal activation procedure. Chemists and engineers employ TPR and published about 3000 articles reporting this characterization. TPR entails the selection of the operative parameters, namely hydrogen concentration in the carrier gas, its flow rate, the amount of samples, and the furnace heating rate. The variable P assesses these parameters. From the value that P takes, engineers evaluate whether the data they read are reproducible and reliable ($P < 20\,\mathrm{K}$). TPR traces depend on the size of the metal aggregates and on the catalyst metal loading. A H_2 conversion from $10\,\%$ to $66\,\%$ minimizes the signal to noise ratio. Raman spectroscopy completes the information that TPR gives and we recommend characterizing a material with both of them in a research paper.

REFERENCES

[1] G. S. Patience, C. A. Patience, F. Bertrand, *Can. J. Chem. Eng.* **2018**, *96*.

[2] S. Robertson, B. McNicol, J. D. Baas, S. Kloet, J. Jenkins, *J. Catal.* **1975**, *37*, 424.

[3] P. Heidebrecht, V. Galvita, K. Sundmacher, *Chem. Eng. Sci.* **2008**, *63*, 4776.

[4] G. S. Patience, Experimental Methods and Instrumentation for Chemical Engineers, 2nd edition, Elsevier B.V., Amsterdam, Netherlands **2017**.

[5] G. S. Patience, *Can. J. Chem. Eng.* **2018**, *96*.

[6] F. Delannay, B. Delmon, Characterization of Heterogeneous Catalysts: Chapter 1. Methods of Catalyst Characterization: An Overview, 1st edition, Marcel Dekker, Inc., New York **1984**.

[7] P. Malet, A. Caballero, *J. Chem. Soc., Faraday Trans. 1* **1988**, *84*, 2369.

[8] Y. Jin, A. K. Datye, *J. Catal.* **2000**, *196*, 8 .

[9] C. Pirola, C. Bianchi, A. D. Michele, P. Diodati, S. Vitali, V. Ragaini, *Catal. Lett.* **2009**, *131*, 294.

[10] C. Pirola, A. D. Fronzo, F. Galli, C. Bianchi, A. Comazzi, F. Manenti, *Chem. Eng. Transactions* **2014**, *37*, 595.

[11] D. Monti, A. Baiker, *J. Catal.* **1983**, *83*, 323.

[12] A. Perianes-Rodriguez, L. Waltman, N. J. van Eck, *J. Informetrics* **2016**, *10*, 1178.

[13] A. Comazzi, C. Pirola, C. L. Bianchi, F. Galli, M. Longhi, F. Manenti, *Can. J. Chem. Eng.* **2016**, *94*, 696.

[14] Z. Dong, H. Zhang, T. Whidden, Y. Zheng, J. Zhao, *Can. J. Chem. Eng.* **2017**, *95*, 1537.

[15] C. G. Visconti, L. Lietti, E. Tronconi, S. Rossini, *Can. J. Chem. Eng.* **2016**, *94*, 685.

[16] J. A. Santander, D. E. Boldrini, M. N. Pedernera, G. M. Tonetto, *Can. J. Chem. Eng.* **2017**, *95*, 1554.

[17] A. B. Jain, P. D. Vaidya, *Can. J. Chem. Eng.* **2016**, *94*, 2364.

[18] S. Gryglewicz, A. Sliwak, J. Cwikla, G. Gryglewicz, *Can. J. Chem. Eng.* **2016**, *94*, 1328.

[19] F. Li, B. Cao, R. Ma, J. Liang, H. Song, H. Song, *Can. J. Chem. Eng.* **2016**, *94*, 1368.

[20] B. Dai, G. Zhou, S. Ge, H. Xie, Z. Jiao, G. Zhang, K. Xiong, *Can. J. Chem. Eng.* **2017**, *95*, 634.

[21] P. K. Sharma, N. Saxena, V. K. Bind, P. K. Roy, A. Bhatt, *Can. J. Chem. Eng.* **2016**, *94*, 752.

[22] M. Chamoumi, N. Abatzoglou, *Can. J. Chem. Eng.* **2016**, *94*, 1801.

[23] V. Rives, M. Ulibarri, A. Montero, *Appl. Clay Sci.* **1995**, *10*, 83.

[24] S. Ansaloni, N. Russo, R. Pirone, *Can. J. Chem. Eng.* **2017**, *95*, 1730.

[25] B. de Caprariis, M. P. Bracciale, P. de Filippis, A. D. Hernandez, A. Petrullo, M. Scarsella, *Can. J. Chem. Eng.* **2017**, *95*, 1745.

[26] K. Nakamura, T. Miyazawa, T. Sakurai, T. Miyao, S. Naito, N. Begum, K. Kunimori, K. Tomishige, *Appl. Catal. B: Environ.* **2009**, *86*, 36.

8

[27] M. Fadoni, L. Lucarelli., *Stud. Surf. Sci. Catal.* **1999**, *120 A*, 177.

[28] L. Lucarelli, *La Chimica e l'industria* **2000**, *82*, 675.

[29] S. Alamolhoda, G. Vitale, A. Hassan, N. N. Nassar, A. P. Pereira, *Can. J. Chem. Eng.* **2018**, *0*.

9